New azole antifungals with a fused triazinone scaffold

David Montoir, Rémi Guillon, Sophie Gazzola, Isabelle Ourliac-Garnier, Kossi Efouako Soklou, Alain Tonnerre, Carine Picot, Aurélien Planchat, Fabrice Pagniez, Patrice Le Pape, Cédric Logé

PII: S0223-5234(20)30049-0

DOI: https://doi.org/10.1016/j.ejmech.2020.112082

Reference: EJMECH 112082

To appear in: *European Journal of Medicinal Chemistry*

Received Date: 14 October 2019

Revised Date: 17 January 2020

Accepted Date: 17 January 2020

Please cite this article as: D. Montoir, Ré. Guillon, S. Gazzola, I. Ourliac-Garnier, K.E. Soklou, A. Tonnerre, C. Picot, Auré. Planchat, F. Pagniez, P. Le Pape, Cé. Logé, New azole antifungals with a fused triazinone scaffold, *European Journal of Medicinal Chemistry* (2020), doi: https://doi.org/10.1016/j.ejmech.2020.112082.

Graphical Abstract

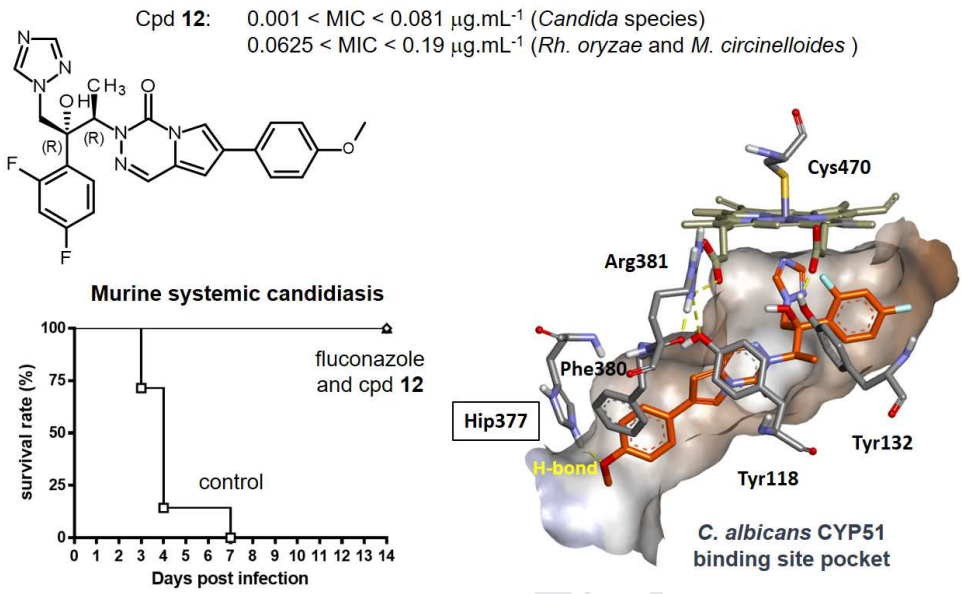

New Azole Antifungals with a Fused Triazinone Scaffold

David Montoir [a], Rémi Guillon [a], Sophie Gazzola [b], Isabelle Ourliac-Garnier [b], Kossi Efouako Soklou [a], Alain Tonnerre [a], Carine Picot [b], Aurélien Planchat [c], Fabrice Pagniez [b], Patrice Le Pape [b], Cédric Logé [a,*].

[a] Université de Nantes, Nantes Atlantique Universités, Département de Chimie Thérapeutique, Cibles et Médicaments des Infections et du Cancer, IICIMED- EA1155, Institut de Recherche en Santé 2, F-44200 Nantes, France

[b] Université de Nantes, Nantes Atlantique Universités, Département de Parasitologie et Mycologie Médicale, Cibles et Médicaments des Infections et du Cancer, IICIMED-EA1155, Institut de Recherche en Santé 2, F-44200 Nantes, France

[c] Université de Nantes, Nantes Atlantique Universités, CEISAM, Chimie et Interdisciplinarité, Synthèse, Analyse, Modélisation, UMR CNRS 6230, Faculté des Sciences et Techniques, F-44322 Nantes, France

* Corresponding author, Département de Chimie Thérapeutique, IICIMED-EA1155, Institut de Recherche en Santé 2, Université de Nantes, 22 boulevard Bénoni Goullin, F-44200 Nantes, France. Tel.: +33 253009154.

E-mail address: cedric.loge@univ-nantes.fr (C. Logé).

Abstract

We identified a new series of azole antifungal agents bearing a pyrrolotriazinone scaffold. These compounds exhibited a broad in vitro antifungal activity against pathogenic *Candida spp*. (fluconazole-susceptible and fluconazole-resistant) and were 10- to 100-fold more active than voriconazole against two *Candida albicans* isolates with known mechanisms of azole resistance (overexpression of efflux pumps and/or specific point substitutions in the Erg11p/CYP51 enzyme). Our lead compound **12** also displayed promising in vitro antifungal activity against some filamentous fungi such as *Aspergillus fumigatus* and the zygomycetes *Rhizopus oryzae* and *Mucor circinelloides*

and an in vivo efficiency against two murine models of lethal systemic infections caused by *Candida albicans*.

Keywords

3*H*-pyrrolo[1,2-*d*][1,2,4]triazin-4-one; Antifungal agents; Azoles; *Candida*; Filamentous fungi; Invasive fungal infections.

1. Introduction

Invasive fungal infections (IFIs) are common and a life-threatening problem in immunocompromised patients. While 90% of all reported fungal-related deaths result from species that belong to one of four genera: *Candida*, *Aspergillus*, *Cryptococcus* and *Pneumocystis*, disseminated infections due to non-*Aspergillus* moulds such as *Rhizopus* spp., *Mucor* spp., *Fusarium* spp. and *Scedosporium* spp. are increasing [1,2,3]. The antifungal armamentarium includes the polyenes (amphotericin B formulations), fluoropyrimidine (flucytosine), echinocandins and the azoles such as fluconazole, itraconazole (first-generation triazoles), voriconazole, posaconazole and isavuconazole (second-generation triazoles). All these compounds differ in their spectrum of activity, pharmacokinetics/pharmacodynamics (PK/PD) properties, indications, dose, safety profile, and cost [4,5]. Among them, the triazoles inhibit cytochrome P450-dependent lanosterol 14α-demethylation (CYP51) leading to a depletion of ergosterol (major component of the fungal cell membrane) and accumulation of 14α-methylated sterols in the fungal cell membrane. All marketed triazoles are also inhibitors and/or substrates of off-target human cytochromes P450 (CYPs), inducing liver toxicity and potential drug-drug interactions (DDIs) in the presence of concomitant medications [6]. Additionally, long-term therapy of azole antifungals for the treatment of candidiasis has led to the emergence of azole-resistant strains of *Candida albicans* and other *Candida* spp., showing the need to develop new more effective antifungals, in particular those able to circumvent resistance phenomena which can be attributed to mutations in *ERG11* gene encoding Erg11p (CYP51), overexpression of *ERG11* or genes encoding membrane transport proteins (CDR1, CDR2, and MDR1), or alterations in cell wall composition [7a-b]. The recent introduction of isavuconazole, administered as a water-soluble prodrug isavuconazonium sulfate, displays high oral bioavailability, linear pharmacokinetics and fewer DDIs compared to voriconazole and posaconazole, but clinical experience is still limited [5]. Other promising investigational compounds VT-1161 and VT-1598 (Viamet Pharmaceuticals, Inc.) bearing a tetrazole moiety with improved fungal CYP51 selectivity compared to human hepatic CYP enzymes [8,9], have been co-crystalized with either *Candida albicans*-CYP51 (CA-CYP51, pdb code: 5TZ1) [10] or *Aspergillus fumigatus*-CYP51B (AF-CYP51B, pdb code: 5FRB) [11]. These structures highlighted the importance of an optimized hydrogen-bonding

interaction with the fungal-specific residue His377 of CA-CYP51 or the corresponding His374 of AF-CYP51B, respectively.

Previously, we have already described the design of a broad-spectrum antifungal agent bearing a linear thiazoloquinazolinone scaffold (compound **I**) [12]. This compound exhibited high in vitro activity against pathogenic *Candida* species and filamentous fungi and showed in vivo antifungal e□cacy in a mice model of systemic candidiasis. To further investigate structure-activity relationships (SAR) in this series, the central scaffold was modified by a fused pyrrolotriazinone moiety, that allows us to increase the size of our molecules by the introduction of a benzene moiety at position 7 (Fig. 1). We suppose that *para*-substitution with hydrogen bond acceptors (HBA) should target the histidine fungal-specific residue, enhance binding for fungal CYP51 and also compensate mutations near the heme site that confer resistance to compact triazoles.

2. Chemistry

The synthesis of newly azoles **6**-**12** was accomplished as depicted in Scheme 1, starting from 1*H*-pyrrole-2-carboxaldehyde **1** which can be brominated with *N*-bromosuccinimide affording 4-bromo-1*H*-pyrrole-2-carboxaldehyde **2** [13]. According to the literature, pyrrolo[1,2-*d*][1,2,4]triazin-4-one **3** can be prepared either by condensation of 1-carbethoxy-2-formylpyrrole with formylhydrazine to give a hydrazone and cyclisation under acidic conditions but with low yield [14], or by condensation of carbethoxyhydrazine with pyrrole-2-carboxaldehyde to give a carbethoxyhydrazone and cyclisation in the presence of sodium propoxide in propanol under reflux conditions for 24h [15]. For this latter condition, Sakai et al. also used a sub-stoichiometric amount of sodium hydride using *N*,*N*-dimethylformamide (DMF) at 100°C for 15h, because the liberated alkoxide ion functioned as a base in the reaction [16]. We applied a similar strategy for the synthesis of compounds **3** and **4**, while exploring the use of microwave activation for our key intermediate 7-bromo derivative (**4**) by changing the solvents (absolute ethanol instead of DMF for the hydrazone synthesis and 1,4-dioxane instead of DMF in the cyclization step), adding a drying work up and changing the amount of sodium hydride (1.1 eq. instead of sub-stoichiometric amount). These modifications resulted in a reduced overall synthesis time (from 15-24 h to less than 2 h), an improved yield (quantitative) and a cleaner reaction. Both these

scaffolds were then condensed into the previously described chiral oxirane **5** (synthesized in 8 steps from (*R*)-methyl lactate) [17] in presence of K_2CO_3 in *N*-methyl-2-pyrrolidone (NMP) at 80°C, to afford compounds **6** and **7** in 49% and 44% yield, respectively. Finally, starting from compound **7**, aromatic moieties were introduced at position 7 under a microwave-assisted Suzuki cross-coupling reactions with various boronic acids. The structure of **9** was confirmed by a single-crystal X-ray diffraction (Fig. 2).

3. Results and discussion

3.1. Biological assays

3.1.1. In vitro antifungal activity

The in vitro antifungal activities of compounds **6**-**12** were compared with those of fluconazole, voriconazole, itraconazole, posaconazole, and amphotericin B against pathogenic *Candida* species (fluconazole-susceptible and fluconazole-resistant) and some filamentous fungi (*Aspergillus* and non-*Aspergillus* moulds). The minimum inhibitory concentration (MIC) values are shown in Tables 1 and 2.

Against the fluconazole-susceptible *Candida albicans* isolate (CAAL93) (Table 1), all these compounds exhibited a high level of activity with MIC values generally below 0.001 $\mu g.mL^{-1}$ (highest MIC value at 0.048 $\mu g.mL^{-1}$), comparable to that observed for voriconazole. Against the two fluconazole-resistant *Candida albicans* isolates with identified mechanisms of resistance (for DSY735: upregulation of the *ERG11* and ABC transporters *CDR1* and *CDR2* genes; for DSY292: mutations G464S, R467K, Y132H in the encoded drug target enzyme Erg11p (CYP51) and overexpression of the multidrug resistance *MDR1* gene) [18,19], compounds bearing 7-aryl substituents (**8**-**12**) were the most active with MIC values 10- to 100-fold lower than that of voriconazole, while the more compact unsubstituted molecule **6** and, to a lesser extent, its bromo derivative **7**, did not significantly improve the antifungal activity. These results demonstrate that our extended compounds are able to bypass the main mechanisms of fluconazole resistance in *C. albicans* (overexpression of efflux pumps and Erg11p (CYP51) as well as certain specific mutations close to the heme site reducing binding affinity for azole). In

addition, a broad-spectrum antifungal activity was also observed more particularly for compounds **8**-**12** against two intrinsically fluconazole-resistant *C. krusei* isolates (CAKR7 and CAKR8) and against a less fluconazole-sensitive *C. glabrata* isolate (CAGL2) with MIC values ranging from 0.008 (for CAGL2) to 0.101 µg.mL^{-1} (for CAKR8).

Among 8 clinical filamentous fungi isolates (Table 2), these compounds showed variable antifungal activities with the lowest MIC values observed for the 7-aryl substituents (**9**-**12**) against some zygomycetes (*Rhizopus orizae* RHPOR1 and RHPOR2 (MIC, 0.0625 to 0.25 µg.mL^{-1}) and *Mucor circinelloides* MURI1 (MIC, 0.19 to 0.75 µg.mL^{-1})), similar to those observed for amphotericin B (the first-line treatment for mucormycosis) [20] and posaconazole, whereas voriconazole lacked any useful activity (MIC, ≥ 8 µg.mL^{-1}). Against some *Aspergillus fumigatus* isolates (itraconazole-susceptible, ASFU7 and ASFU76 or -resistant, ASFU77), the antifungal activity of compounds **9** and **12** was less effective than that seen against Mucorales with MIC values on the µg.mL^{-1} range, even if these compounds are only 10-fold less active than voriconazole (usually the first-line agent for the treatment of invasive aspergillosis) [21]. Against a clinical isolate of *Scedosporium apiospermum* (SCAP1), only compounds **7** and **12** displayed moderate MIC values on the µg.mL^{-1} range, but nevertheless close to those observed for itraconazole and voriconazole (MIC, 0.5 µg.mL^{-1}) which typically have the lowest MIC value among the antifungal drugs [22]. Finally, none of these compounds showed significant antifungal activities against a clinical isolate of a *Fusarium* sp. (FU sp.), a species which often display high levels of resistance to existing antifungal agents and are some of the more difficult fungi to treat [23]. Based on all these biological results, compound **12** was selected for further testing.

3.1.2. Sterol analysis

The mechanism of action of this series was investigated by studying inhibition of *C. albicans* CAAL93 ergosterol biosynthesis after treatment by compound **12**. As shown in Table 3, 32% of ergosterol biosynthesis inhibition was obtained with a concentration of 1.0 ng.mL^{-1} corresponding to the MIC value. At a 10-fold higher concentration, a dose-dependent effect was observed causing 53% ergosterol biosynthesis inhibition. This significant reduction of ergosterol and the concomitant accumulation of 14α-methylated

precursors lanosterol and eburicol, in a dose-dependent manner, indicated that compound **12** interfered with sterol 14α-demethylase cytochrome P450 (CYP51).

3.1.3. Acute oral toxicity study in rats

Treatment of rats with compound **12** by an oral route at a dose level of 300 mg/kg bw did not cause mortality during the 14 days of observation. This dose level caused hunched back and slightly decreased activity in all the experimental animals but all of them were symptom free the next day after treatment. In addition, this study showed no indication of a test item-related effect concerning body weight gain and was not associated with any macroscopic findings. The method used was not intended to allow the calculation of a precise LD50 value, but according to the Globally Harmonized Classification System (GHS) criteria [24], compound **12** can be ranked as "Category 4" for acute oral exposure.

3.1.4. In vivo antifungal activity

Two murine models of lethal systemic *Candida* infection were developed to evaluate the in vivo efficacy of antifungal compound **12** (Fig. 4). After a tail injection of *C. albicans* blastoconidia with the fluconazole-susceptible isolate (CAAL93), all control mice died within 7 days while the groups treated with 10 mg/kg fluconazole or compound **12** showed 100% survival after 14 days (Fig. 4A). A significant reduction in kidney fungal burden (Log(CFU)/gram of tissue) compared to control was also observed for fluconazole and compound **12** ($p<0.0001$). In the disseminated *Candida* infection model caused by a fluconazole- and voriconazole-resistant isolate (DSY292) (Fig. 4B), all control mice or those treated with 15 mg/kg fluconazole died within 5 days ($p=0.4110$) or within 8 days for those treated with voriconazole ($p=0.0054$), while the group treated with 15 mg/kg compound **12** were still alive 10 days post infection ($p<0.0001$). However, these mice were suddenly in a moribund state and, due to ethical rules, required euthanasia to avoid animal suffering. Furthermore, in this assay, kidneys of mice treated with compound **12** demonstrated a significant decrease of fungal burden compared to control, fluconazole and voriconazole groups ($p<0.0001$). Although a significant increase of survival and a significant decrease of tissue burden was observed, further optimization concerning pharmacokinetic/pharmacodynamic (PK/PD)

characteristics of compound **12** could be performed by increasing doses or prolonging the duration of exposure to this antifungal.

3.2. Molecular modeling

Docking analysis of compound **12** into the active site pocket of CA-CYP51 (Fig. 5) showed a hydrogen-bonding interaction between the imidazole side chain of fungal-specific residue His377 and the methoxy group of the molecule, in addition to many other van der Waals / aromatic interactions including Tyr118, Leu121, Phe126, Ile131, Tyr132, Phe228, Phe233, Pro230, Leu376, Phe380 and Met508. Since all compounds bearing 7-aryl substituents (**8**-**12**) are strongest *C. albicans* CYP51 inhibitors against isolate DSY292 which have mutations near the heme site, compared to the more compact molecules **6**, voriconazole and fluconazole (Table 1), we can support the importance of such hydrophobic extended side chains in the stabilization of the inhibitors with the protein moieties. The importance of residue His377 is not clear as equivalent biological activities were observed in all *C. albicans* isolates, even if such an interaction may contribute to reinforce both affinity and specificity of these antifungals within the active site.

4. Conclusion

In summary, we have synthesized a new series of triazole antifungal agents with a pyrrolotriazinone scaffold. Our lead compound **12** significantly reduced mortality rates and kidney fungal burden in two murine models of lethal systemic infections due to fluconazole-susceptible or fluconazole- and voriconazole-resistant isolates and showed promising in vitro antifungal activity against some filamentous fungi such as *Aspergillus fumigatus* and the zygomycetes *Rhizopus oryzae* and *Mucor circinelloides*. The mechanism of action for this antifungal against *C. albicans* was confirmed by sterol analyses and is characteristic of an in vitro CYP51 inhibition. Further studies on this series will focus on developing murine models of invasive pulmonary aspergillosis (IPA) and mucormycosis, which are among the most common life-threatening mould complications in immunocompromised patients, but also on the determination of their

binding affinity with human CYP enzymes, as drug-drug interactions (DDIs) still represent a major “Achilles’ heel” for most azoles in clinical use.

5. Experimental section

5.1. General remarks

Melting points were determined using an Electrothermal IA9300 digital melting point apparatus and reported uncorrected. IR absorption spectra were recorded on a MIRacle Shimatzu spectrometer. NMR spectra were recorded on Bruker Avance 400 spectrometer (^{1}H NMR at 400 MHz and ^{13}C NMR at 100 MHz). Chemical shifts are expressed as δ values (ppm) relative to tetramethylsilane as internal standard (in NMR description, s = singlet, d = doublet, t = triplet, q = quadruplet, m = multiplet and bs = broad signal). Coupling constants *J* are given in Hertz (Hz). All reactions were monitoring by thin layer chromatography (TLC) using commercially available plates Alugram® Xtra SIL G/UV254 (0.20 mm). Focused microwave irradiations were carried out with a CEM Discover™ focused microwave reactor (300W, 2455 MHz, monomode system). Silica gel column chromatography was carried out with Macherey-Nagel Silica gel 60 (0.063-0.2 mm). Reverse-phase flash column chromatography was performed on a BUCHI Grace Reveleris® X2 apparatus using Chromabond® flash RS 120 C18 cartridges. Electrospray mass spectrometric analyses were performed on a Waters Acquity UPLC system ZQ 2000 single quadrupole spectrometer. Formic acid (0.1%) was added in diluent to improve ionization. All tested compounds displayed more than 97% purity as determined using this analytical LC-MS system (TIC and UV). High resolution mass spectra were obtained by ESI/TOF. The optical rotations were recorded with a polarimeter Schmidt-Haensch Polartronic NH8. Chemicals and solvents used were commercially available. Optically oxirane (2*R*,3*S*) **5** was synthesized according to protocol described in Ref. [17] ($[\alpha]^{20}_{D}$ = -9.0 (c = 1.0 in MeOH) (lit: $[\alpha]^{20}_{D}$ = -8.3)).

5.2. Chemistry

*5.2.1. 4-Bromo-1H-pyrrole-2-carboxaldehyde (**2**).*

To a stirred solution of 1*H*-pyrrole-2-carboxaldehyde **1** (1 g, 10.52 mmol) in acetonitrile (10 mL) at 0°C was added *N*-bromosuccinimide (1.872 g, 10.52 mmol) and the solution was stirred at 0°C for 15 minutes. Water was added and the resulting mixture was extracted with diethyl ether. Organic layers were dried over anhydrous Na_2SO_4, filtered and concentrated in vacuo. Crystallization of the crude mixture using cyclohexane/ethanol afforded compound **2** as white crystals (1.125 g, 60%): R_f=0.22 (CH_2Cl_2); mp: 121-122 °C (lit.[13] mp: 120°C); ^{1}H NMR (400 MHz, DMSO-d_6): δ 7.12 (m, 1H), 7.41 (m, 1H), 9.48 (s, 1H), 12.51 (bs, 1H); ^{13}C NMR (100 MHz, DMSO-d_6): δ 97.0, 120.8, 126.5, 132.9, 179.1; IR (cm^{-1}): 3238, 3108, 2926, 2860, 1655, 1380, 1357, 1147, 1104, 920, 827, 771, 744, 598; MS (ESI) *m/z* 173.9 (95) ^{79}Br[M+H]$^+$; 175.9 (95) ^{81}Br[M+H]$^+$.

*5.2.2. 3H-Pyrrolo[1,2-d][1,2,4]triazin-4-one (**3**).*

To a stirred solution of ethyl carbazate (241 mg, 2.31 mmol) in *N*,*N*-dimethylformamide (5 mL) was added 1*H*-pyrrole-2-carboxaldehyde (**1**) (200 mg, 2.10 mmol) and the solution was stirred at 90°C for 24 h. The solution was cooled to 0°C, sodium hydride (60% dispersion in mineral oil) (42 mg, 1.05 mmol) was added and the reaction mixture was stirred at 90°C for 24 h. Water was added and the resulting mixture was extracted with ethyl acetate. Organic layers were washed with brine, dried over anhydrous Na_2SO_4, filtered and concentrated in vacuo. The residue was purified on silica gel column chromatography (petroleum ether/diethyl ether 7:3) to yield compound **3** as a white powder (172 mg, 60%): R_f=0.31 (Petroleum ether/Et_2O 1:1); mp: 160-161 °C (lit.[15] mp: 169°C); ^{1}H NMR (400 MHz, DMSO-d_6): δ 6.86 (m, 2H), 7.79 (m, 1H), 8.28 (s, 1H), 12.29 (bs, 1H); ^{13}C NMR (100 MHz, DMSO-d_6): δ 109.1, 115.4, 116.2, 125.6, 132.4, 144.7; IR (cm^{-1}): 3238, 3200, 3100, 2996, 2935, 1718, 1602, 1438, 1421, 1352, 1313, 1260, 1215, 1163, 1081, 875, 762, 732, 626; MS (ESI) *m/z* 135.8 (100) [M+H]$^+$.

*5.2.3. 7-Bromo-3H-pyrrolo[1,2-d][1,2,4]triazin-4-one (**4**).*

To a stirred solution of ethyl carbazate (329 mg, 3.16 mmol) in absolute ethanol (17 mL) was added 1*H*-pyrrole-2-carboxaldehyde (**1**) (500 mg, 2.87 mmol) and the solution

was exposed to microwave irradiation for 5 min at 105°C using maximal microwave power up to 200 W. After completion, the solvent was evaporated to dryness; the residue was dissolved in ethyl acetate (20 mL), dried over Na_2SO_4, filtered and the filtrate was evaporated to dryness. Sodium hydride (60% dispersion in mineral oil) (128.7 mg, 3.22 mmol) was added portionwise to a solution of the obtained residue in anhydrous dioxane (17 mL) and the mixture was stirred at room temperature for 45 min. Afterwards the mixture was irradiated for 1 h at 140°C using microwave system operating at maximal microwave power up to 200W. Solvent was evaporated to dryness and the residue was quenched with a saturated aqueous solution of NH_4Cl (55 mL), water (5 mL) and extracted with ethyl acetate (3×120 mL). The aqueous phase was extracted with ethyl acetate (2×120 mL) after saturation with NaCl (crystals). Organic layers were dried over anhydrous Na_2SO_4, filtered and concentrated in vacuo. The residue was purified on silica gel column chromatography (CH_2Cl_2/EtOH 99:1) to yield compound **4** as a grey powder (424 mg, 69%): R_f=0.24 (CH_2Cl_2/EtOH 99:1); mp: 187-188 °C; ^{1}H NMR (400 MHz, DMSO-d_6): δ 6.95 (d, 1H, ^4J=1.6 Hz), 7.93 (d, 1H, ^4J=1.6 Hz), 8.21 (s, 1H), 12.44 (bs, 1H); ^{13}C NMR (100 MHz, DMSO-d_6): δ 104.4, 110.6, 115.8, 126.3, 131.3, 143.3; IR (cm^{-1}): 3203, 3151, 3102, 1717, 1533, 1474, 1409, 1383, 1327, 1302, 1147, 891, 825, 727, 628; MS (ESI) *m/z* 213.9 (66) ^{79}Br[M+H]$^+$; 215.9 (51) ^{81}Br[M+H]$^+$; UPLC purity 99%.

*5.2.4. 3-[(1R,2R)-2-(2,4-Difluorophenyl)-2-hydroxy-1-methyl-3-(1,2,4-triazol-1-yl) propyl]-3H-pyrrolo[1,2-d][1,2,4]triazin-4-one (**6**).*

To a stirred solution of (2*R*,3*S*)-2-(2,4-difluorophenyl)-3-methyl-2-[(1*H*-1,2,4-triazol-1-yl)methyl]oxirane **5** (279 mg, 1.11 mmol) in *N*-methyl-2-pyrrolidone (3 mL) was added K_2CO_3 (113 mg, 0.81 mmol) and 3*H*-pyrrolo[1,2-*d*][1,2,4]triazin-4-one **3** (100 mg, 0.74 mmol). The solution was stirred at 80°C for 24 h. Mixture was diluted with water and product was extracted with ethyl acetate. Organic layers were dried over anhydrous Na_2SO_4 and concentrated in vacuo. The residue was purified on silica gel column chromatography (Et_2O) to yield compound **6** as a white powder (140 mg, 49%): R_f=0.10 (Et_2O); mp: 131-132 °C; $[\alpha]^{20}_D$ = +30.0 (c = 0.1 in MeOH); ^{1}H NMR (400 MHz, DMSO-d_6): δ 1.20 (d, 3H, ^3J=6.8 Hz), 4.46 (d, 1H, ^2J=14.4 Hz), 4.90 (d, 1H, ^2J=14.4 Hz), 5.61-5.68 (m, 2H), 6.89-6.98 (m, 3H), 7.23 (m, 1H), 7.33 (m, 1H), 7.58 (s, 1H),

7.87 (s, 1H), 8.27 (s, 1H), 8.47 (s, 1H); ^{13}C NMR (100 MHz, DMSO-d_6): δ 14.1, 54.7, 55.5, 77.4, 103.9 (dd, $^{2}J_{C\text{-}F}$=$^{2}J_{C\text{-}F}$=28.0 Hz), 109.6, 110.9 (d, $^{2}J_{C\text{-}F}$=20.0 Hz), 116.0, 117.5, 124.0 (d, $^{2}J_{C\text{-}F}$=13.0 Hz), 125.0, 130.0 (dd, $^{3}J_{C\text{-}F}$=$^{3}J_{C\text{-}F}$=7.0 Hz), 132.7, 144.7, 145.0, 150.2, 158.7 (d, $^{1}J_{C\text{-}F}$=245.0 Hz), 161.9 (d, $^{1}J_{C\text{-}F}$=245.0 Hz); IR (cm^{-1}): 3398, 3126, 1706, 1676, 1617, 1598, 1499, 1448, 1424, 1344, 1272, 1164, 1139, 963, 732, 682; MS (ESI) *m/z* 387.1 (100) $[M+H]^+$; UPLC purity 100%. HRMS (ESI): calcd. for $C_{18}H_{16}N_6O_2F_2$ $[M+H]^+$ 387.1377, found: 387.1376.

*5.2.5. 7-Bromo-3-[(1R,2R)-2-(2,4-difluorophenyl)-2-hydroxy-1-methyl-3-(1,2,4-triazol-1-yl)propyl]-3H-pyrrolo[1,2-d][1,2,4]triazin-4-one (**7**).*

According to the synthesis of 3-[(1*R*,2*R*)-2-(2,4-difluorophenyl)-2-hydroxy-1-methyl-3-(1*H*-1,2,4-triazol-1-yl)propyl]pyrrolo[1,2-*d*][1,2,4]triazin-4-one **6** starting from (2*R*,3*S*)-2-(2,4-difluorophenyl)-3-methyl-2-[(1*H*-1,2,4-triazol-1-yl)methyl]oxirane **5** (880 mg, 3.51 mmol) and 7-bromo-3*H*-pyrrolo[1,2-*d*][1,2,4]triazin-4-one **4** (500 mg, 2.34 mmol). The residue was purified by reverse-phase flash column chromatography (water/acetonitrile 98:2 + formic acid 0.1% → 10 mn → acetonitrile + formic acid 0.1%) to yield compound **7** as a beige powder after lyophilization and trituration in diisopropyl ether (480 mg, 44%): R_f=0.27 (CH_2Cl_2/EtOH 98:2); mp: 142-143 °C; $[\alpha]^{20}_D$ = +20.0 (c = 0.1 in MeOH); ^{1}H NMR (400 MHz, DMSO-d_6): δ 1.22 (d, 3H, ^{3}J=7.2 Hz), 4.50 (d, 1H, ^{2}J=14.4 Hz), 4.89 (d, 1H, ^{2}J=14.4 Hz), 5.50-5.70 (m, 2H), 6.96 (ddd, 1H, $^{3}J_{H\text{-}F}$=$^{3}J_{H\text{-}H}$=8.4 Hz, $^{4}J_{H\text{-}H}$=2.6 Hz), 7.06 (d, 1H, ^{4}J=1.2 Hz), 7.24 (ddd, 1H, $^{3}J_{H\text{-}F}$=$^{3}J'_{H\text{-}F}$=9.2 Hz, $^{4}J_{H\text{-}H}$=2.6 Hz), 7.34 (m, 1H), 7.60 (s, 1H), 8.05 (d, 1H, ^{4}J=1.2 Hz), 8.27 (s, 1H), 8.43 (s, 1H); ^{13}C NMR (100 MHz, DMSO-d_6): δ 14.1, 54.7, 55.9, 77.4, 103.9 (dd, $^{2}J_{C\text{-}F}$=$^{2}J_{C\text{-}F}$=28.0 Hz), 104.8, 111.0, 111.1, 117.0, 124.0, 125.7, 130.0 (dd, $^{3}J_{C\text{-}F}$=$^{3}J_{C\text{-}F}$=9.0 Hz), 131.5, 143.7, 144.7, 150.2, 158.7 (d, $^{1}J_{C\text{-}F}$=245.0 Hz), 161.9 (d, $^{1}J_{C\text{-}F}$=245.0 Hz); IR (cm^{-1}): ν=3376, 3159, 1706, 1617, 1499, 1458, 1401, 1329, 1294, 1272, 1173, 1133, 1043, 961, 852, 727, 670; MS (ESI) *m/z* 465.0 (94) ^{79}Br$[M+H]^+$; 466.9 (100) ^{81}Br$[M+H]^+$; UPLC purity 100%. HRMS (ESI): calcd. for $C_{18}H_{15}N_6O_2F_2Br$ $[M+H]^+$ 465.0492, found: 465.0481.

*5.2.6. 3-[(1R,2R)-2-(2,4-Difluorophenyl)-2-hydroxy-1-methyl-3-(1,2,4-triazol-1-yl)propyl]-7-phenyl-3H-pyrrolo[1,2-d][1,2,4]triazin-4-one (**8**).*

To a 10 mL vial were added under argon 7-bromo-3-[(1*R*,2*R*)-2-(2,4-difluorophenyl)-2-hydroxy-1-methyl-3-(1,2,4-triazol-1-yl)propyl]-3*H*-pyrrolo[1,2-*d*][1,2,4]triazin-4-one **7** (200 mg, 0.43 mmol), benzeneboronic acid (61 mg, 0.43 mmol), $Pd(PPh_3)_4$ (25 mg, 0.05 mmol), 2M Na_2CO_3 aqueous solution (2 mL) and acetonitrile (2 mL). The resulting mixture was exposed to microwave irradiation for 10 min at 120°C using maximal microwave power up to 100 W. The reaction mixture was cooled to room temperature and diluted with water. Product was extracted with methylene chloride, organic layers were dried over anhydrous Na_2SO_4 and concentrated in vacuo. The residue was purified on silica gel column chromatography (CH_2Cl_2 and CH_2Cl_2/EtOH 99:1) to yield compound **8** as a green powder (119 mg, 60%): R_f=0.29 (CH_2Cl_2/EtOH 98:2); mp: 146-147 °C; $[\alpha]^{20}_D$ = +80.0 (c = 0.1 in MeOH); ^{1}H NMR (400 MHz, DMSO-d_6): δ 1.20 (d, 3H, ^3J=6.8 Hz), 4.48 (d, 1H, ^2J=14.4 Hz), 4.89 (d, 1H, ^2J=14.4 Hz), 5.60-5.67 (m, 2H), 6.92 (ddd, 1H, $^3J_{H-F}$=$^3J_{H-H}$=8.4 Hz, $^4J_{H-H}$=2.4 Hz), 7.21 (m, 1H), 7.27-7.37 (m, 3H), 7.43 (dd, 2H, $^3J_{H-H}$=7.2 Hz; $^3J_{H-H}$=8.0 Hz), 7.56 (s, 1H), 7.85 (d, 2H, $^3J_{H-H}$=7.2 Hz), 8.26 (s, 1H), 8.33 (s, 1H), 8.44 (s, 1H); ^{13}C NMR (100 MHz, DMSO-d_6): δ 14.1, 54.8, 55.5, 77.4, 104.0 (dd, $^2J_{C-F}$=$^2J_{C-F}$=28.0 Hz), 106.7, 111.0 (d, $^2J_{C-F}$=21.0 Hz), 113.9, 124.1 (d, $^2J_{C-F}$=16.0 Hz), 125.9, 126.0 (2C), 127.6, 129.0 (2C), 130.1, 130.7, 132.5, 132.7, 144.7, 144.8, 150.2, 158.7 (d, $^1J_{C-F}$=245.0 Hz), 161.9 (d, $^1J_{C-F}$=245.0 Hz); IR (cm^{-1}): ν=3403, 1696, 1617, 1500, 1458, 1408, 1272, 1210, 1133, 1045, 964, 851, 758, 728, 677, 511; MS (ESI) *m/z* 463.1 (100) $[M+H]^+$; UPLC purity 100%. HRMS (ESI): calcd. for $C_{24}H_{20}N_6O_2F_2$ $[M+H]^+$ 463.1687, found: 463.1689.

*5.2.7. 7-(4-Chlorophenyl)-3-[(1R,2R)-2-(2,4-difluorophenyl)-2-hydroxy-1-methyl-3-(1,2,4-triazol-1-yl)propyl]-3H-pyrrolo[1,2-d][1,2,4]triazin-4-one (**9**).*

According to the synthesis of 3-[(1*R*,2*R*)-2-(2,4-difluorophenyl)-2-hydroxy-1-methyl-3-(1,2,4-triazol-1-yl)propyl]-7-phenyl-3*H*-pyrrolo[1,2-*d*][1,2,4]triazin-4-one **8** starting from 7-bromo-3-[(1*R*,2*R*)-2-(2,4-difluorophenyl)-2-hydroxy-1-methyl-3-(1,2,4-triazol-1-yl)propyl]-3*H*-pyrrolo[1,2-*d*][1,2,4]triazin-4-one **7** (200 mg, 0.43 mmol) and 4-chlorobenzeneboronic acid (61 mg, 0.43 mmol) to yield compound **9** as a light yellow powder (98 mg, 46%): R_f=0.25 (CH_2Cl_2/EtOH 98:2); mp: 204-205 °C; $[\alpha]^{20}_D$ = +30.0 (c = 0.1 in MeOH); ^{1}H NMR (400 MHz, DMSO-d_6): δ 1.20 (d, 3H, ^3J=6.8 Hz), 4.48 (d, 1H, ^2J=14.4 Hz), 4.88 (d, 1H, ^2J=14.4 Hz), 5.55-5.67 (m, 2H), 6.93 (m, 1H), 7.22 (m,

1H), 7.28-7.35 (m, 2H), 7.48 (d, 2H, $^{3}J_{H\text{-}H}$=8.8 Hz), 7.56 (s, 1H), 7.89 (d, 2H, $^{3}J_{H\text{-}H}$=8.8 Hz), 8.25 (s, 1H), 8.38 (s, 1H), 8.44 (s, 1H); ^{13}C NMR (100 MHz, DMSO-d_6): δ 14.1, 54.8, 55.8, 77.5, 103.9 (dd, $^{2}J_{C\text{-}F}$=$^{2}J_{C\text{-}F}$=27.0 Hz), 106.7, 111.0 (d, $^{2}J_{C\text{-}F}$=18.0 Hz), 114.3, 124.1 (d, $^{3}J_{C\text{-}F}$=9.0 Hz), 126.0, 126.7, 127.8 (2C), 128.9 (2C), 129.4, 130.1, 131.7, 132.1, 132.5, 144.7, 150.2, 158.7 (d, $^{1}J_{C\text{-}F}$=245.0 Hz), 161.9 (d, $^{1}J_{C\text{-}F}$=245.0 Hz); IR (cm^{-1}): ν=3386, 1707, 1599, 1500, 1386, 1293, 1269, 1179, 1138, 1091, 825, 677, 519; MS (ESI) *m/z* 497.1 (100) ^{35}Cl[M+H]$^{+}$, 499.1 (39) ^{37}Cl[M+H]$^{+}$; UPLC purity 97%. HRMS (ESI): calcd. for $C_{24}H_{19}N_6O_2F_2Cl$ [M+H]$^{+}$ 497.1313, found: 497.1299.

*5.2.8. 3-[(1R,2R)-2-(2,4-Difluorophenyl)-2-hydroxy-1-methyl-3-(1,2,4-triazol-1-yl)propyl]-7-(4-nitrophenyl)-3H-pyrrolo[1,2-d][1,2,4]triazin-4-one (**10**).*

According to the synthesis of 3-[(1*R*,2*R*)-2-(2,4-difluorophenyl)-2-hydroxy-1-methyl-3-(1,2,4-triazol-1-yl)propyl]-7-phenyl-3*H*-pyrrolo[1,2-*d*][1,2,4]triazin-4-one **8** starting from 7-bromo-3-[(1*R*,2*R*)-2-(2,4-difluorophenyl)-2-hydroxy-1-methyl-3-(1,2,4-triazol-1-yl)propyl]-3*H*-pyrrolo[1,2-*d*][1,2,4]triazin-4-one **7** (200 mg, 0.43 mmol) and 4-nitrobenzeneboronic acid (72 mg, 0.43 mmol). The residue was purified on silica gel column chromatography (petroleum ether/ethyl acetate 60:40) followed by reverse-phase flash column chromatography (water/acetonitrile 98:2 + formic acid 0.1% → 10 mn → acetonitrile + formic acid 0.1%) to yield compound **10** as a brown powder after lyophilization and trituration in diisopropyl ether (51 mg, 47%): R_f=0.25 (CH_2Cl_2/EtOH 98:2); mp: 130-131 °C; $[\alpha]^{20}_{D}$ = +50.0 (c = 0.1 in MeOH); ^{1}H NMR (400 MHz, DMSO-d_6): δ 1.20 (d, 3H, ^{3}J=7.2 Hz), 4.50 (d, 1H, ^{2}J=14.4 Hz), 4.88 (d, 1H, ^{2}J=14.4 Hz), 5.57-5.70 (m, 2H), 6.94 (ddd, 1H, $^{3}J_{H\text{-}F}$=$^{3}J_{H\text{-}H}$=8.4 Hz, $^{4}J_{H\text{-}H}$=2.4 Hz), 7.22 (m, 1H), 7.31 (m, 1H), 7.46 (s, 1H), 7.56 (s, 1H), 8.16 (d, 2H, $^{3}J_{H\text{-}H}$=8.8 Hz), 8.24 (s, 1H), 8.26 (d, 2H, $^{3}J_{H\text{-}H}$=8.8 Hz), 8.48 (s, 1H), 8.59 (s, 1H); ^{13}C NMR (100 MHz, DMSO-d_6): δ 14.0, 54.7, 55.8, 77.4, 103.9 (dd, $^{2}J_{C\text{-}F}$=$^{2}J_{C\text{-}F}$=27.0 Hz), 107.0, 111.0 (d, $^{2}J_{C\text{-}F}$=20.0 Hz), 115.9, 124.0, 124.2 (2C), 126.3, 126.9 (2C), 128.3, 130.1, 132.6, 139.6, 144.6, 144.7, 146.4, 150.2, 158.6 (dd, $^{1}J_{C\text{-}F}$=245.0 Hz, $^{3}J_{C\text{-}F}$=12.0 Hz), 161.9 (dd, $^{1}J_{C\text{-}F}$=245.0 Hz, $^{3}J_{C\text{-}F}$=12.0 Hz); IR (cm^{-1}): ν=3448, 1701, 1509, 1342, 1212, 1132, 964, 852, 752; MS (ESI) *m/z* 508.0 (100) [M+H]$^{+}$; UPLC purity 98%.

*5.2.9. 4-{3-[(1R,2R)-2-(2,4-Difluorophenyl)-2-hydroxy-1-methyl-3-(1,2,4-triazol-1-yl)propyl]-4-oxo-3,4-dihydro-pyrrolo[1,2-d][1,2,4]triazin-7-yl}benzonitrile (**11**).*

According to the synthesis of 3-[(1*R*,2*R*)-2-(2,4-difluorophenyl)-2-hydroxy-1-methyl-3-(1,2,4-triazol-1-yl)propyl]-7-phenyl-3*H*-pyrrolo[1,2-*d*][1,2,4]triazin-4-one **8** starting from 7-bromo-3-[(1*R*,2*R*)-2-(2,4-difluorophenyl)-2-hydroxy-1-methyl-3-(1,2,4-triazol-1-yl)propyl]-3*H*-pyrrolo[1,2-*d*][1,2,4]triazin-4-one **7** (200 mg, 0.43 mmol) and 4-cyanobenzeneboronic acid (63 mg, 0.43 mmol). The residue was purified on silica gel column chromatography (methylene chloride/ethanol 99:1 and diethyl ether/ethyl acetate 80:20) to yield compound **11** as a light yellow powder (105 mg, 50%): R_f=0.23 (CH_2Cl_2/EtOH 98:2); mp: 201-202 °C; $[\alpha]^{20}_D$ = +20.0 (c = 0.1 in MeOH); ^{1}H NMR (400 MHz, DMSO-d_6): δ 1.20 (d, 3H, ^3J=6.8 Hz), 4.48 (d, 1H, ^2J=14.6 Hz), 4.88 (d, 1H, ^2J=14.6 Hz), 5.50-5.72 (m, 2H), 6.92 (m, 1H), 7.20 (m, 1H), 7.31 (m, 1H), 7.42 (s, 1H), 7.55 (s, 1H), 7.88 (d, 2H, $^3J_{H-H}$=8.0 Hz), 8.07 (d, 2H, $^3J_{H-H}$=8.0 Hz), 8.24 (s, 1H), 8.45 (s, 1H), 8.53 (s, 1H); ^{13}C NMR (100 MHz, DMSO-d_6): δ 14.1, 54.7, 55.8, 77.4, 103.9 (dd, $^2J_{C-F}$=$^2J_{C-F}$=28.0 Hz), 106.9, 109.8, 111.0 (d, $^2J_{C-F}$=22.0 Hz), 115.5, 118.9, 124.0, 126.2, 126.7 (2C), 128.8, 130.1, 132.6, 132.9 (2C), 137.6, 144.7, 150.2, 157.4, 160.8 (1C not visible); IR (cm^{-1}): ν=3447, 2221, 1699, 1500, 1388, 1293, 1138, 1047, 966, 804; MS (ESI) *m/z* 488.1 (100) $[M+H]^+$; UPLC purity 100%.

*5.2.10. 3-[(1R,2R)-2-(2,4-Difluorophenyl)-2-hydroxy-1-methyl-3-(1,2,4-triazol-1-yl)propyl]-7-(4-methoxyphenyl)-3H-pyrrolo[1,2-d][1,2,4]triazin-4-one (**12**).*

According to the synthesis of 3-[(1*R*,2*R*)-2-(2,4-difluorophenyl)-2-hydroxy-1-methyl-3-(1,2,4-triazol-1-yl)propyl]-7-phenyl-3*H*-pyrrolo[1,2-*d*][1,2,4]triazin-4-one **8** starting from 7-bromo-3-[(1*R*,2*R*)-2-(2,4-difluorophenyl)-2-hydroxy-1-methyl-3-(1,2,4-triazol-1-yl)propyl]-3*H*-pyrrolo[1,2-*d*][1,2,4]triazin-4-one **7** (350 mg, 0.75 mmol) and 4-methoxybenzeneboronic acid (114 mg, 0.75 mmol). The residue was purified on silica gel column chromatography (dichloromethane/ethyl acetate 96:4), then triturated in diethyl ether to yield after filtration compound **12** as a yellow powder (218 mg, 59%): R_f=0.29 (CH_2Cl_2/EtOH 98:2); mp: 172-173 °C; $[\alpha]^{20}_D$ = +20.0 (c = 0.1 in MeOH); ^{1}H NMR (400 MHz, DMSO-d_6): δ 1.19 (d, 3H, ^3J=6.8 Hz), 3.78 (s, 3H), 4.47 (d, 1H, ^2J=14.6 Hz), 4.88 (d, 1H, ^2J=14.6 Hz), 5.55-5.70 (m, 2H), 6.92 (m, 1H), 6.98 (d, 2H, $^3J_{H-H}$=8.8 Hz), 7.21 (m, 1H), 7.25 (d, 1H, $^4J_{H-H}$=1.6 Hz), 7.30 (m, 1H), 7.55 (s, 1H),

7.77 (d, 2H, $^{3}J_{H\text{-}H}$=8.8 Hz), 8.22 (s, 1H), 8.25 (s, 1H), 8.41 (s, 1H); ^{13}C NMR (100 MHz, DMSO-d_6): δ 14.1, 54.8, 55.2 (2C), 77.4, 103.9, 106.5, 111.1, 113.0, 114.4, 124.2, 125.2, 125.8 (2C), 127.3 (2C), 130.0, 130.6, 132.4, 144.7, 150.2, 158.9 (1C + 2CF not visible); IR (cm^{-1}): ν=3447, 1700, 1616, 1500, 1428, 1407, 1387, 1298, 1250, 1180, 1134, 1029, 959, 808, 723; MS (ESI) *m/z* 493.3 (100) $[M+H]^+$; UPLC purity 100%. HRMS (ESI): calcd. for $C_{25}H_{22}N_6O_3F_2$ $[M+H]^+$ 493.1805, found: 493.1794.

5.3. Crystallographic analysis

Single crystals of compound **9** suitable for X-ray diffraction were prepared by slow diffusion of diethyl ether through a saturated solution of the product in dichloromethane. The crystal was mounted at the tip of Lindemann capillary by means of a solvent free glue. The intensity measurement was carried out at 293 K on a Bruker-Nonius Kappa CCD diffractometer, using graphite-monochromatized Mo*K*-$L_{2,3}$ radiation (λ = 0.71073 Å) up to a resolution of $(\sin\theta/\lambda)_{max}$ = 0.64 Å^{-1}. The structure was solved using the charge flipping algorithm [25] implemented in the Superflip program [26] and refined with JANA2006 program [27] against F^2 for all reflections. Non-hydrogen atoms were refined with anisotropic displacement parameters. All H atoms were introduced in geometrically optimized positions and refined with a riding model, except for alcohol H atom, which position was determined by difference Fourier. CCDC-1857098 contains the supplementary crystallographic data. These data can be obtained free of charge from the Cambridge Crystallographic Data Centre via www.ccdc.cam.ac.uk/data_request/cif.

Crystal data: $C_{24}H_{19}Cl_1F_2N_6O_2$, Mr = 496.9, tetragonal, $P4_32_12$, a = 11.4927(10), b = 11.4927 (10), c = 34.328(5) Å, V = 4534.1(9) Å3, Z =8, ρ_{calcd} = 1.4559 g.cm^{-3}, μ = 0.221 mm^{-1}, F(000) = 2048, prism, 0.22 × 0.21 × 0.08 mm^3, T = 293 K, 25530 reflections, 4865 unique (99% completeness), 320 parameters, GOF = 1.51, wR2 = 0.1659, R = 0.0919 for 2431 reflections with I > 2σ(*I*).

5.4. Biology

5.4.1. Antifungal drugs

Fluconazole, voriconazole, itraconazole, posaconazole and amphotericin B powders were purchased from Sigma-Aldrich, St Quentin Fallavier, France.

5.4.2. In vitro antifungal activity

Candida spp.

Candida spp. suspensions were prepared in RPMI 1640 medium (Sigma, Saint Quentin Fallavier, France) supplemented with 0.165 M morpholinopropanesulphonic acid (MOPS, Sigma), 2% glucose and antibiotics and adjusted to give a final concentration of 10^3 cells mL^{-1}. A 96-well microplate (Nunc, Dutscher SA, France) was seeded with 100 µL of *Candida* suspension. Molecules were first dissolved in dimethylsulfoxide (except fluconazole in water) and then diluted in culture medium. Each concentration of molecule (100 µL) to be tested was added and plates were incubated at 37 °C for 24 h. The cellular viability was evaluated spectrofluorometrically with an excitation at 550 nm and an emission at 590 nm after a 4 h incubation with 10 µL of resazurin (Interchim, Montluçon, France) [28]. The minimal inhibitory concentration (MIC) is the concentration that inhibited 50% of the cell growth. MICs were determined by linear regression analysis.

Aspergillus fumigatus

Conidia of *A. fumigatus* were microscopically counted and diluted in RPMI 1640 medium (Sigma) supplemented with 0.165 M morpholinopropanesulphonic acid (MOPS, Sigma), 2% glucose and antibiotics. One hundred microliters of a 10^4 cells mL^{-1} suspension were inoculated in a 96-well microplate (Nunc). Drugs were prepared as described for *Candida spp.* evaluations and 100 µL of the drug dilutions were added to the cell suspension. After an incubation time of 48 h at 37 °C, the cellular viability was evaluated as in *Candida* assay after an incubation time of 20h with resazurin [28]. Activity of the studied and reference molecules was expressed as the MIC. The MIC is the concentration that inhibited 80% of the cell growth. MICs were determined by linear regression analysis.

Other filamentous fungi

The broth microdilution test was done in accordance with the CLSI guidelines for filamentous fungi (CLSI document M38) [29] using RPMI 1640 medium (Sigma) buffered to pH 7.0 with MOPS (Sigma). Drugs were diluted in DMSO and further in culture medium. Final drug range was 0.032-16 mg/L. Stock inoculum suspensions were prepared from 7-day-old cultures grown on potato dextrose agar following the CLSI guidelines (document M38-A3). Stock suspensions contained conidia or sporangiospores. The diluted (2×) inoculum sizes ranged from 0.9×10^4 to 4.7×10^4 CFU/mL. Drug-free and cell-free controls were included. The microdilution plates were incubated at 35°C and read after 48 h except for the Zygomycetes, which were read at 24 h. The MIC endpoints were read visually with the aid of a reading mirror and expressed as the lowest drug concentration that prevented 100% growth.

5.4.3. Sterol extraction and analysis

To study sterol synthesis, *C. albicans* CAAL93 blastospores were incubated in 50 mL Sabouraud broth medium (Sigma-Aldrich) during 18 hours at 35° C with stirring. Fluconazole and compound **12** were introduced into culture medium before incubation. Cells were collected by centrifugation at 1500 g. Pellet was suspended in 3 mL of fresh ethanolic potassium hydroxide solution (25 g of KOH, 36 mL of distilled water and brought to100 mL with 100 % ethanol). Saponification was performed at 80°C for 60 min. Sterols were extracted by addition of 3 mL of hexane and the organic phase was then washed by adding 1 mL of sterile water. Final organic phase was transferred to a new collection tube after 5 min centrifugation step at 2000 rpm. An equivalent of 50 mg mycelia was transferred into a glass tube and 2.5 µg of cholesterol was added as internal standard. Hexane was evaporated by heating at 80°C. Sterols were derivatized with 100 µL of *N*-Methyl-*N*-(trimethylsilyl)trifluoroacetamide (TMS) (Sigma-Aldrich) during 30 min at room temperature. The solvent was then evaporated at 80°C. Dried sterols were solubilized with 200 µL dichloromethane and stored at -20°C until analysis.

Sterols as TMS derivatives were analyzed by GC-MS using an Agilent 7890A GC system, with a SLB-5^{TM} column (30 m × 0.25 mm, 0.25 µm, Sigma-Aldrich, France) coupled with a mass detector (Agilent 5975C inert MSD – E.I. 70 eV). One microliter of sample was injected in splitless mode at 250 °C. The carrier gas was helium at a flow

rate of 1 mL/min. The oven was set at 150°C for 0.5 min and then raised to 290 °C at 50 °C/min and from 290 °C to 305 °C at 2 °C/min. Sterols were identified via their electron ionization fragmentation pattern, compared to published data. Results are expressed as percent area of total sterols. Relative Retention Time are expressed as the ratio between retention of sterol and retention time of cholesterol.

5.4.4. Acute oral toxicity study

Evaluation of acute oral toxicity of compound **12** was conducted by CiToxLab Hungary Ltd. (study code: 15/276-001P) according to the acute toxic class method (OECD 423 and Commission Regulation (EC) No 440/2008 of 30 May 2008, B.1.Tris) [30,31] in two groups of three female CRL:(WI) rats. The test substance, synthesized by Diverchim (Roissy, France; DIV07169 (i.e. compound **12**), batch No. 404-193-Es2, >99% purity UV), was administered by gavage at a dose level of 300 mg/kg bw (Group 1 and Group 2). General behavioral observations, body weight changes, signs of toxicity, and mortality were recorded at 30 minutes, 1, 2, 4 and 6 hours after dosing and daily for 14 days thereafter. All animals were sacrificed by exsanguination under pentobarbital anesthesia. After examination of the external appearance, the cranial, thoracic and the abdominal cavities were opened and the organs and the tissues were observed. Macroscopic abnormalities were recorded.

5.4.5. Animal use and care

Swiss mice (Janvier Labs, Le Genest-Saint-Isle, France) with a body weight of ~25 g were obtained and allowed to acclimate for 7 days prior to use. Environmental controls for the animal room were set to maintain a temperature of 16 to 22°C, a relative humidity of 30 to 70%, and a 12:12 hourly light-dark cycle. All the experimental protocols were prior approved by the Ethic Committee on Animal Testing (comité d'éthique en expérimentation animale N°006) and was authorized by the French Ministry of Higher Education, Research and Innovation (APAFIS≠9710-2017042410186554 v4).

5.4.6. Systemic C. albicans infection models

Mice were immunodepressed by subcutaneous injection of 30 mg/kg prednisolone (Hydrocortancyl®) one day before challenge. On day 0, mice were infected intravenously (100 µL) with a suspension of fluconazole susceptible *C. albicans* (CAAL93) or both fluconazole- and voriconazole-resistant *C. albicans* (DSY292) blastoconidia (5.10^6 yeast/mL). One hour after infection, mice were treated *per os* once daily with 10 mg/kg (for CAAL93) or 15 mg/kg (for DSY292) body weight of compound **12**, fluconazole or voriconazole solubilized in 40% DMSO, 25% tween80 and 35% olive oil for 5 consecutive days. The control group received 100 µL of 40% DMSO, 25% tween80 and 35% olive oil. To prevent rapid clearance of the molecules, all animals were given 50% grapefruit juice (*ad libitum*) instead of water 5 days before infection until the end of the treatment period [32]. Survival was monitored for 14 days post inoculation. Differences in cohorts were analyzed by the log-rank Mantel Cox test. Kidneys of mice euthanized on ethically considerations or at the end of the assay (day 14) were excised and weighed. Tissues were homogenized and serially diluted 10- to 1000-fold in sterile saline, then plated onto Sabouraud dextrose agar and incubated for 48 h to determine the number of colony-forming units (CFUs). Tissue fungal burden was expressed as average Log(CFU)/gram of tissue. Differences in mean CFUs in kidneys were compared with the vehicle control using a one-way ANOVA with a post-hoc Tukey test. For both tests, survival and tissue burden, a P value of <0.05 was considered statistically significant.

5.5. Molecular modeling

Molecular modeling studies were performed using SYBYL-X 1.3 software [33] running on a Dell precision T3400 workstation. The three-dimensional structure of compound **12** was built from a standard fragments library and optimized using the Tripos force field [34] including the electrostatic term calculated from Gasteiger and Hückel atomic charges. Powell's method available in Maximin2 procedure was used for energy minimization until the gradient value was smaller than 0.001 kcal/(mol*Å). The crystal structure of sterol 14-alpha demethylase from *C. albicans* (CA-CYP51) in complex with posaconazole at 2.86 Å resolution (pdb code: 5FSA) [10] was used as template for docking. Water molecules were removed from the coordinates set since no information

about conserved water molecules is known for this chemical series in CA-CYP51. Flexible docking of compound **12** into the binding site was performed using GOLD software [35]. The most stable docking model was selected according to the best scored conformation predicted by the GoldScore scoring function. Finally, the complexe was energy-minimized using Powell's method available in Maximin2 procedure with the Tripos force field and a dielectric constant of 4.0, until the gradient value reached 0.1 kcal/mol.Å. Biovia Discovery Studio Visualizer [36] was used for graphical display.

Declaration of interest

The authors declare the following financial interests/personal relationships which may be considered as potential competing interests: C. Logé, R. Guillon, D. Montoir, F. Pagniez and P. Le Pape have a patent granted (WO 2017/020944 A1), "Novel fused pyrimidinone and triazinone derivatives, their process of preparation and their therapeutic uses as antifungal and/or antiparasitic agents" published on February 9th, 2017.

Acknowledgments

We thank Pr. Dominique Sanglard (Institute of Microbiology, University of Lausanne, Switzerland) for providing strains DSY735 and DSY292 used in this study, and Dr. Catherine Roullier (University of Nantes, France) for the HRMS measurements. This work was supported by a grant from SATT Ouest Valorisation.

Supplementary materials

Electronic Supplementary Information (ESI) available: spectroscopic data (UPLC-MS, HRMS, ^{1}H and ^{13}C) for representative compounds.

References

[1] G.D. Brown, D.W. Denning, N.A. Gow, S.M. Levitz, M.G. Netea, T.C. White, Hidden killers: human fungal infections, Sci. Transl. Med. 4 (2012) 165rv13.

[2] R. Lester, J.H. Rex, Fungaemia and disseminated infection, in: C.C. Kibbler, R. Barton, N.A.R. Gow, S. Howell, D.M. MacCallum, R.J. Manuel (Eds.), Oxford Textbook of Medical Mycology, Oxford: Oxford University Press, 2018, pp. 163-170.

[3] A.P. Douglas, S.C. Chen, M.A. Slavin, Emerging infections caused by non-Aspergillus filamentous fungi, Clin. Microbiol. Infect. 22 (2016) 670-680.

[4] D.P. Kontoyiannis, Invasive mycoses: Strategies for effective management, Am. J. Med. 125 (2012) S25–S38.

[5] N. Spernovasilis, D.P. Kofteridis, Pre-existing liver disease and toxicity of antifungals, J. Fungi (Basel) 4 (2018) E133.

[6] A. Mourad, J.R. Perfect, Tolerability profile of the current antifungal armoury, J. Antimicrob. Chemother. 73 (2018) i26-i32.

[7] (a) J. Beardsley, C.L. Halliday, S.C. Chen, T.C. Sorrell, Responding to the emergence of antifungal drug resistance: perspectives from the bench and the bedside, Future Microbiol. 13 (2018) 1175-1191; (b) L.E. Cowen, D. Sanglard, S.J. Howard, P.D. Rogers, D.S. Perlin, Mechanisms of antifungal drug resistance, Cold Spring Harb. Perspect. Med. 5 (2014) a019752.

[8] C.M. Yates, E.P. Garvey, S.R. Shaver, R.J. Schotzinger, W.J. Hoekstra, Design and optimization of highly-selective, broad spectrum fungal CYP51 inhibitors, Biorg. Med. Chem. Lett. 27 (2017) 3243-3248.

[9] J. Zhang, L. Li, Q. Lv, L. Yan, Y. Wang, Y. Jiang, The fungal CYP51s: their functions, structures, related drug resistance, and inhibitors, Front. Microbiol. 10 (2019) 691.

[10] T.Y. Hargrove, L. Friggeri, Z. Wawrzak, A. Qi, W.J. Hoekstra, R.J. Schotzinger, Structural analyses of *Candida albicans* sterol 14alpha-demethylase complexed with azole drugs address the molecular basis of azole-mediated inhibition of fungal sterol biosynthesis, J. Biol. Chem. 292 (2017) 6728-6743.

[11] T.Y. Hargrove, E.P. Garvey, W.J. Hoekstra, C.M. Yates, Z. Wawrzak, G. Rachakonda, F. Villalta, G.I. Lepesheva, Crystal structure of the new investigational drug candidate VT-1598 in complex with *Aspergillus fumigatus*

679 sterol 14α-demethylase provides insights into its broad-spectrum antifungal
680 activity, Antimicrob. Agents Chemother. 61 (2017) e00570-17.
681 [12] R. Guillon, F. Pagniez, C. Picot, D. Hédou, A. Tonnerre, E. Chosson, M. Duflos,
682 T. Besson, C. Logé, P. Le Pape, Discovery of a novel broad-spectrum antifungal
683 agent derived from albaconazole, ACS Med. Chem. Lett. 4 (2013) 288-292.
684 [13] M. Krayer, T. Balasubramanian, C. Ruzié, M. Ptaszek, D.L. Cramer, M.
685 Taniguchi, J.S. Lindsey, Refined syntheses of hydrodipyrrin precursors to chlorin
686 and bacteriochlorin building blocks, J. Porphyrins Phthalocyanines 13 (2009)
687 1098-1110.
688 [14] C. Jaureguiberry, B. Roques, Synthesis of pyrrolo[1,2-d]triazines, CR Acad. Sci.
689 (Paris) 274(C) (1972) 1703-1706.
690 [15] J.-C. Lancelot, D. Maume, M. Robba, Pyrrolo[1,2-d]triazines. II. Study of
691 pyrrolo[1,2-d]triazin-1-ones and -4-ones, J. Heterocyclic Chem. 17 (1980) 631-
692 635.
693 [16] N. Sakai, M. Funabashi, T. Hamada, S. Minakata, I. Ryu, M. Komatsu, Synthesis
694 of mesomeric betaines containing a pyrrolo- or imidazotriaziniumolate system and
695 their cycloaddition with acetylenic dipolarophiles leading to triazocinone
696 derivatives, Tetrahedron 55 (1999) 13703-13724.
697 [17] A. Tasaka, N. Tamura, Y. Matsushita, K. Teranishi, R. Hayashi, K. Okonogi, K.
698 Itoh, Optically active antifungal azoles. I. Synthesis and antifungal activity of
699 (2*R*,3*R*)-2-(2,4-difluorophenyl)-3-mercapto-1-(1*H*-1,2,4-triazol-1-yl)-2-butanol
700 and its stereoisomers, Chem. Pharm. Bull. 41 (1993) 1035-1041.
701 [18] A. Coste, A. Selmecki, A. Forche, D. Diogo, M.E. Bougnoux, C. d'Enfert, J.
702 Berman, D. Sanglard, Genotypic evolution of azole resistance mechanisms in
703 sequential Candida albicans isolates, Eukaryot. Cell 6 (2007) 1889-1904.
704 [19] N. Dunkel, J. Blass, P.D. Rogers, J. Morschhäuser, Mutations in the multi-drug
705 resistance regulator MRR1, followed by loss of heterozygosity, are the main cause
706 of MDR1 overexpression in fluconazole-resistant Candida albicans strains, Mol.
707 Microbiol. 69 (2008) 827-840.
708 [20] N.V. Sipsas, M.N. Gamaletsou, A. Anastasopoulou, D.P. Kontoyiannis. Therapy
709 of Mucormycosis, J. Fungi (Basel) 4 (2018) pii: E90.

[21] J.D. Jenks, M. Hoenigl. Treatment of Aspergillosis. J. Fungi (Basel) 4 (2018) pii: E98.

[22] M.W. McCarthy, A. Katragkou, E. Losifidis, E. Roilides, T. J. Walsh, Recent advances in the treatment of Scedoporiosis and Fusariosis, J. Fungi (Basel) 4 (2018) pii: E73.

[23] A. Lupetti, R. Danesi, M. Campa, M.D. Tacca, S. Kelly, Molecular basis of resistance to azole antifungals, Trends Mol. Med. 8 (2002) 76–81.

[24] Globally Harmonised System of Classification and Labelling of Chemicals (GHS), sixth revised ed., UN, New York and Geneva, 2015.

[25] G. Oszlanyi, A. Süto, Ab initio structure solution by charge flipping, Acta Crystallogr. A. 60 (2004) 134-141.

[26] L. Palatinus, G. Chapuis, Superflip - a computer program for the solution of crystal structures by charge flipping in arbitrary dimensions, J. Appl. Cryst. 40 (2007) 786-790.

[27] V. Petricek, M. Dusek, L. Palatinus, Crystallographic Computing System JANA2006: General features, Z. Kristallogr. 229 (2014) 345-352.

[28] F. Pagniez, P. Le Pape, New fluorometric screening test for possible antifungal drugs, J. Mycol. Med. 11 (2001) 73-78.

[29] Clinical and Laboratory Standards Institute. Reference method for broth dilution antifungal susceptibility testing of filamentous fungi; Approved standard, 3rd ed., CLSI document M38, Clinical and Laboratory Standards Institute, Wayne, PA 2017.

[30] OECD guidelines for testing of chemicals No. 423. Acute oral toxicity - Acute toxic class method. Adopted: 17 December 2001.

[31] Commission regulation (EC) No 440/2008 of 30 May 2008, B.1. Tris.

[32] A.M. Sugar, X.P. Liu, Effect of grapefruit juice on serum voriconazole concentrations in the mouse, Med. Mycol., 38 (2000) 209-212.

[33] SYBYL-X 1.3, Tripos Associates, Inc. 1699 South Hanley Road, St. Louis, MO 63144, U.S.A.

[34] M. Clarck, R.D. Cramer III, N. Van Opdenbosch, Validation of the general purpose tripos 5.2 force field, J. Comput. Chem. 10 (1989), 982-1012.

[35] G. Jones, P. Willet, R.C. Glen, Development and validation of a genetic algorithm for flexible docking, J. Mol. Biol. 267 (1997) 727-748.

[36] Dassault Systèmes BIOVIA, Discovery Studio Visualizer, v19.1.0.18287, San Diego: Dassault Systèmes, 2018.

748 **Fig. 1.** General structures of synthesized compounds.
749

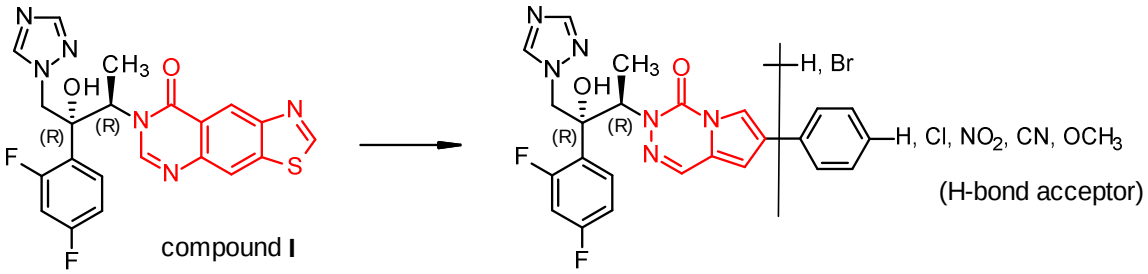

750
751
752
753
754
755

Fig. 2. ORTEP view of compound **9**.

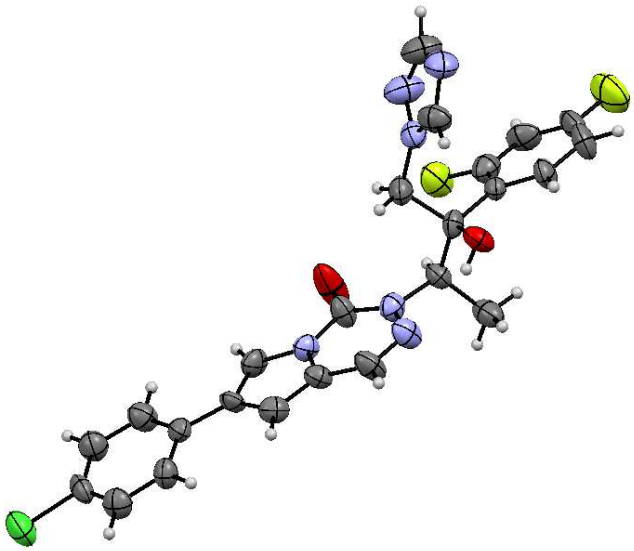

Scheme 1. Synthesis of compounds **6-12**. Reagents and conditions: (*i*) NBS (1 eq), CH_3CN, 0°C, 15 min, 60%; (*ii*) For R=H: a) $H_2NNHCOOEt$ (1.1 eq), DMF, 90°C, 24 h; b) NaH (60% dispersion in mineral oil, 0.5eq), DMF, 90°C, 24 h, 60%; For R=Br: a) $H_2NNHCOOEt$ (1.1 eq), EtOH, 105°C (MW), 5' then drying work up; b) NaH (60% dispersion in mineral oil, 1.1 eq), 1,4-dioxane (anhydrous), rt, 45 min, then 140°C (MW), 1h, quantitative; (*iii*) oxirane (2R,3S) **5** (1.5 eq), K_2CO_3 (1.1 eq), NMP, 80°C, 24 h, 44-49%; (*iv*) starting from cpd **7**: Ar-$B(OH)_2$ (1 eq), $Pd(PPh_3)_4$ (0.12 eq), ACN, Na_2CO_3 (2M), 120°C (MW), 10', 46-60%.

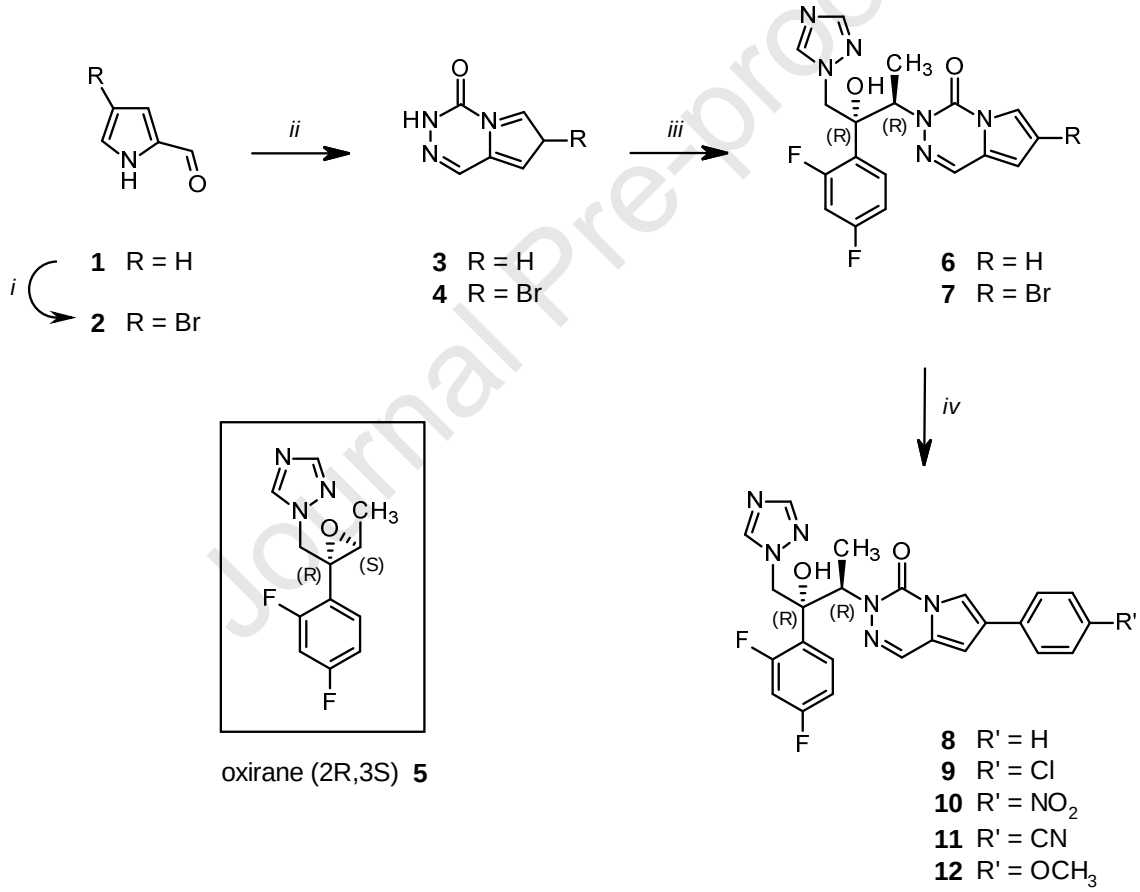

Table 1

Susceptibilities of clinical isolates of Candida species to compounds **6-12** and reference antifungal agents.

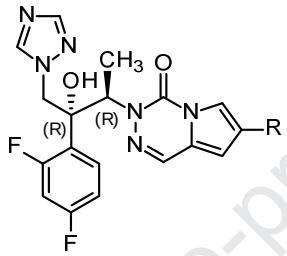

Cpd	R	MIC values (µg.mL^{-1})[a]					
		CAAL93	DSY735	DSY292	CAKR7	CAKR8	CAGL2
6	H	< 0.001	0.48±0.199	0.79±0.092	0.625±0.057	1.15	0.099±0.004
7	Br	0.002±0.0004	0.14±0.012	0.155±0.005	0.251±0.079	0.076±0.002	0.014±0.001
8	C_6H_5	< 0.001	0.016±0.001	0.014±0.002	0.013±0.001	0.014	0.008±0.005
9	(*p*)Cl-C_6H_4	< 0.001	0.018±0.005	0.014±0.001	0.019±0.001	0.079	0.061±0.008
10	(*p*)NO_2-C_6H_4	< 0.001	0.017±0.007	0.018±0.001	0.066±0.009	0.039±0.027	0.074±0.038
11	(*p*)CN-C_6H_4	< 0.048	n.d.	0.016±0.001	0.058±0.009	0.101±0.014	0.025±0.010
12	(*p*)OCH_3-C_6H_4	< 0.001	< 0.001	0.018±0.002	0.062±0.032	0.081±0.009	0.017±0.003
FLC		0.036±0.02	> 30	> 3	> 3	> 10	10.10±0.61
VOR		0.005±0.001	0.458±0.196	1.1±0.1	0.817±0.007	0.24±0.07	0.126±0.003

[a]Values represent the mean±SD of experiments performed in triplicate. *Candida albicans* (CAAL93, DSY735, DSY292), *Candida krusei* (CAKR7, CAKR8) and *Candida glabrata* (CAGL2). Fluconazole (FLC), voriconazole (VOR). n.d.: not determined. CAAL93: fluconazole-susceptible *Candida albicans* isolate. DSY735: fluconazole-resistant *Candida albicans* isolate with upregulation of the *ERG11* and ABC transporters *CDR1* and *CDR2* genes. DSY292: fluconazole-resistant *Candida albicans* isolate with mutations G464S, R467K, Y132H in Erg11p (CYP51) and overexpression of the multidrug resistance *MDR1* gene.

Table 2

Susceptibilities of clinical isolates of filamentous fungi to compounds **6-12** and reference antifungal agents.

Cpd	R	MIC values (µg.mL^{-1})[a]							
		ASFU7	ASFU76	ASFU77	RHPOR1	RHPOR2	MURI1	FU sp.	SCAP1
6	H	24.31±9.57	18.12±10.10	52.75±4.54	4*	8*	16*	> 16	> 16
7	Br	6.99±1.01	6.66±0.14	6.74±0.26	4*	8*	8*	> 16	4.0±0.0
8	C_6H_5	44.06±7.76	48.41±7.95	64.80±7.46	n.d.	n.d.	n.d.	n.d.	n.d.
9	(*p*)Cl-C_6H_4	6.07±0.05	6.21±0.18	9.27±1.05	0.19±0.09	0.125±0.0	0.19±0.09	> 16	> 16
10	(*p*)NO_2-C_6H_4	8.31±0.052	8.23±2.23	> 100	0.0625±0.0	0.25±0.0	0.25±0.0	12.0±5.65	> 16
11	(*p*)CN-C_6H_4	>100	>100	>100	0.125±0.0	0.25±0.0	0.75±0.35	10.0±8.48	> 16
12	(*p*)OCH_3-C_6H_4	2.21±0.09	6.52±0.16	6.60±0.24	0.0625±0.0	0.094±0.04	0.19±0.09	> 16	3.0±1.14
VOR		0.15±0.001	0.64±0.01	0.61±0.04	n.d.	8.0±0.0	> 8	6.0±2.84	0.5±0.0
ITRA		0.42±0.04	0.50±0.24	> 100	0.19±0.09	1.125±1.124	0.19±0.09	> 16	0.5±0.0
POSA		n.d.	n.d.	n.d.	0.19±0.09	0.5±0.0	0.19±0.09	> 8	1.25±1.06
Ampho B		n.d.	n.d.	n.d.	0.19±0.09	0.5±0.0	0.19±0.09	12.0±5.65	> 8

[a]Values represent the mean±SD of experiments performed in triplicate (ASFU) or in duplicate (RHPOR, MURI1, FU sp., SCAP1) - excepted * (tested once). *Aspergillus fumigatus* (ASFU76, ASFU7, ASFU77), *Rhizopus orizae* (RHPOR1, RHPOR2), *Mucor* circinelloides (MURI1), *Fusarium sp*. (FU sp.), *Scedosporium apiospermum* (SCAP1). Voriconazole (VOR), itraconazole (ITRA), posaconazole (POSA), amphotericin B (Ampho B). n.d.: not determined.

Table 3

Effect of compound **12** on the sterol composition of *C. albicans* CAAL93.

Sterols[a]	RRT	untreated	**FLC** (ng.mL^{-1})	**12** (ng.mL^{-1})	
			10.0	1.0	10.0
zymosterol	1.08	1.6	2.8	3.3	nd
ergosterol	1.1	89.7	57.8	61.0	42.0
fecosterol	1.15	nd	2.8	3.2	nd
14α-methylfecosterol	1.17	nd	2.0	nd	3.6
ergosta-dienol (5,7 or 5,8)	1.18	1.6	3.2	3.7	1.1
episterol	1.2	2.0	8.8	11.0	nd
lanosterol	1.24	1.6	13.1	7.7	25.2
eburicol	1.31	nd	2.2	1.8	23.1
Other sterols (<1%)		3.5	7.3	8.3	5.0

[a]Relative sterol composition (%) of *C. albicans* (CAAL93) in basal condition (untreated) and after 24h exposure to fluconazole (FLC - 10.0 ng.mL^{-1}) or compound **12** (1.0 and 10.0 ng.mL^{-1}). n.d.: not detected. RRT: relative retention time expressed as the following ratio: RRT = $RT_{sterol}/RT_{cholesterol}$.

Fig. 4. Effect on mice survival and kidney burden of compounds **12**, fluconazole and voriconazole against systemic infection caused by fluconazole-susceptible *C. albicans* (CAAL93) (A) and by fluconazole- and voriconazole-resistant *C. albicans* (DSY292) (B) in neutropenic mice. All compounds were administered orally once a day for 5 days at a dose of 10 mg/kg (for CAAL93) or 15 mg/kg (for DSY292). *n* = 8. Symbols: □, vehicle; ◊, compound **12**; Δ, fluconazole; and ●, voriconazole.

(A) (B)

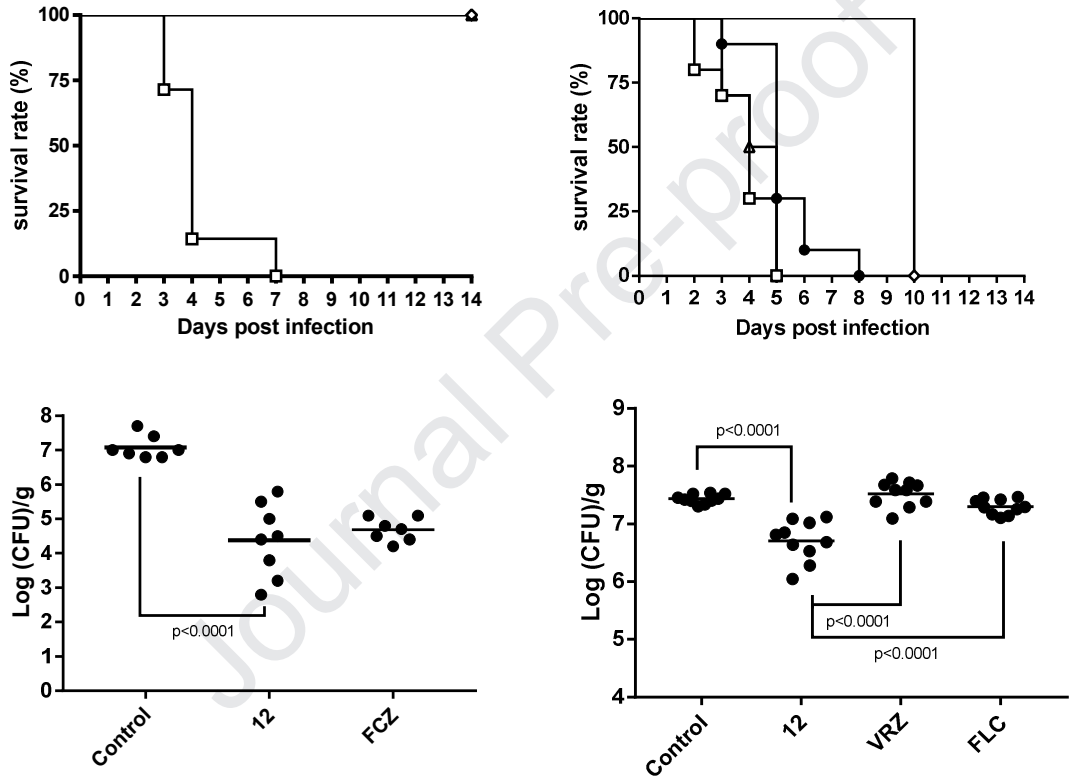

Fig. 5. Binding pose found by the docking program GOLD for compound **12** into the binding site pocket of CYP51-*Candida albicans* (5FSA.pdb). Hip377 is the protonated form of histidine residue. Hydrogen bonds are indicated as yellow lines.

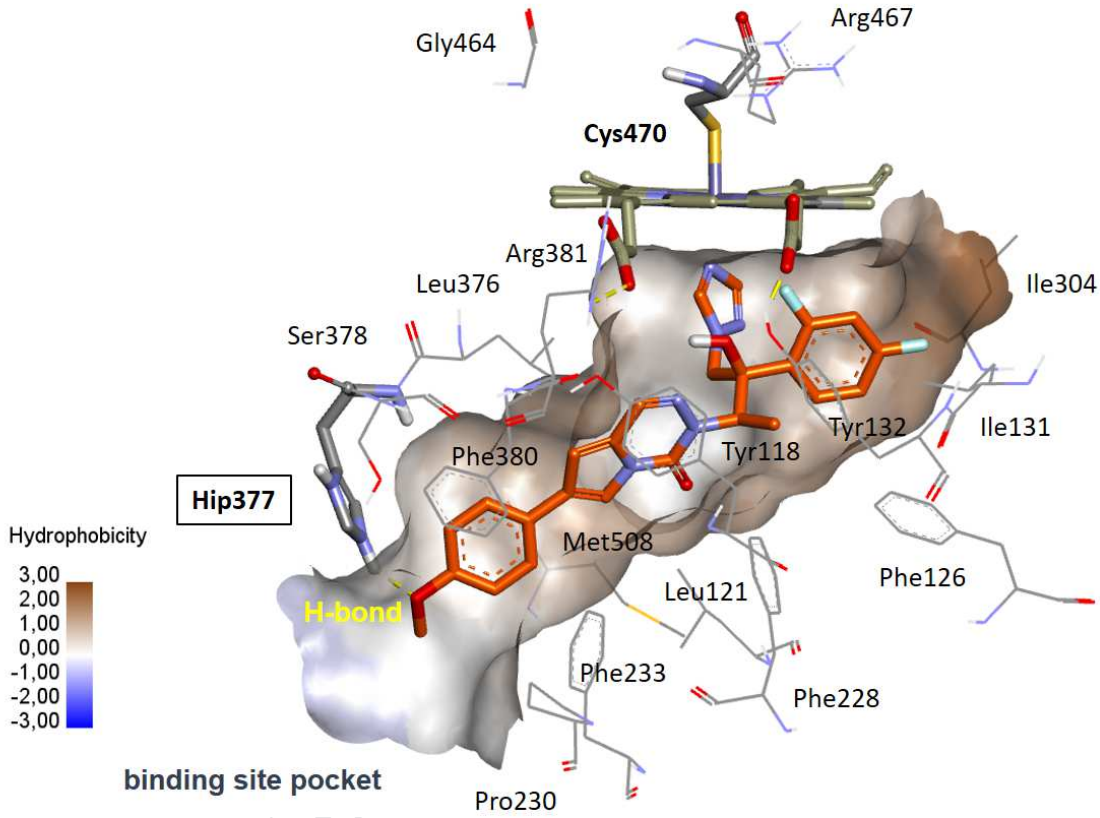

Highlights

- New triazole antifungal agents with a pyrrolotriazinone scaffold (lead compound **12**)

- In vitro antifungal activity against *Candida spp*. (fluconazole- and voriconazole-resistant) and filamentous fungi (*Aspergillus fumigatus* and some zygomycetes)

- In vivo antifungal efficiency in two lethal systemic infections caused by *C. albicans* (fluconazole- and voriconazole-resistant)

Declaration of interests

☒ The authors declare that they have no known competing financial interests or personal relationships that could have appeared to influence the work reported in this paper.

☐The authors declare the following financial interests/personal relationships which may be considered as potential competing interests:

Dr. Cédric Logé